

## Universal Dynamics of Rogue Waves in a Quenched Spinor Bose Condensate

Ido Siovitz<sup>1</sup>, Stefan Lannig<sup>1</sup>, Yannick Deller, Helmut Strobel, Markus K. Oberthaler<sup>1</sup>, and Thomas Gasenzer<sup>1\*</sup>

*Kirchhoff-Institut für Physik, Ruprecht-Karls Universität Heidelberg,  
Im Neuenheimer Feld 227, 69120 Heidelberg, Germany*



(Received 2 May 2023; accepted 10 October 2023; published 2 November 2023)

Isolated many-body systems far from equilibrium may exhibit scaling dynamics with universal exponents indicating the proximity of the time evolution to a nonthermal fixed point. We find universal dynamics connected with the occurrence of extreme wave excitations in the mutually coupled magnetic components of a spinor gas which propagate in an effectively random potential. The frequency of these rogue waves is affected by the time-varying spatial correlation length of the potential, giving rise to an additional exponent  $\delta_c \simeq 1/3$  for temporal scaling, which is different from the exponent  $\beta_V \simeq 1/4$  characterizing the scaling of the correlation length  $\ell_V \sim t^{\beta_V}$  in time. As a result of the caustics, i.e., focusing events, real-time instanton defects appear in the Larmor phase of the spin-1 system as vortices in space and time. The temporal correlations governing the instanton occurrence frequency scale as  $t^{\delta_c}$ . This suggests that the universality class of a nonthermal fixed point could be characterized by different, mutually related exponents defining the evolution in time and space, respectively. Our results have a strong relevance for understanding pattern coarsening from first principles and potential implications for dynamics ranging from the early Universe to geophysical dynamics and microphysics.

DOI: [10.1103/PhysRevLett.131.183402](https://doi.org/10.1103/PhysRevLett.131.183402)

*Introduction.*—The study of quantum dynamics far from equilibrium has been of particular interest in recent years. The time evolution of a system on its way to equilibrium is a rich play field upon which one can examine various dynamical characteristics, including, e.g., prethermalization [1,2], wave turbulence [3,4], superfluid turbulence [5,6], and self-similar spatiotemporal scaling dynamics at a nonthermal fixed point [7–11]. During recent years, studies of such phenomena have intensified, in experiment [12–26] and theory [27–60], many of them in the field of cold gases.

The concept of nonthermal fixed points aims at generalizing upon the description and classification of critical physics in and near equilibrium [61–64] to quenched systems far from equilibrium. The approach of the system to a nonthermal fixed point is reflected by the self-similar spatiotemporal scaling of the order-parameter correlations [9–11]. For example, in coarsening and phase ordering kinetics [65–67], the emergence of scaling evolution is, generically, associated with nonlinear and topological excitations emerging in a system during its ordering evolution. The dynamics of such excitations gives rise to a characteristic length scale in the system, which then typically changes in time according to a power law,  $\ell_\Lambda(t) \sim t^{\beta_\Lambda}$ , with a universal scaling exponent  $\beta_\Lambda$ .

Caustics, the phenomenon of dynamical wave focusing in random media [68–72], may lead to the formation of wave events of extreme amplitude known as (linear) rogue or freak waves [73]. When propagating in a random medium, the flow of waves branches [73–77], resulting

in the repetitive occurrence of new rogue waves. Theoretical investigations of this phenomenon connect spatial and temporal scales, making it an appropriate framework for investigating spatiotemporal scaling phenomena also in nonlinear media [77–81] in which rogue waves are known to occur as specific nonlinear solutions [82,83]. This framework is of great significance in, e.g., the formation of tsunamis in the ocean and structure formation in the early Universe.

*Main result.*—We consider a one-dimensional spin-1 Bose gas, in which the interactions give rise to a variety of nonlinear and topological excitations. We study the spatiotemporal pattern of excitations of the Bose fields  $\Psi_{m_F} = |\Psi_{m_F}| \exp(i\varphi_{m_F})$  of the  $m_F = 0, \pm 1$  magnetic components in the  $F = 1$  hyperfine manifold, after a sudden quench from the polar into the easy-plane phase [84]. Rogue-wave textures are observed to occur as the result of caustics [73–77] of phase excitations, which effectively propagate in a disordered medium with time-varying correlations formed by the respective other components. We find the mean time  $t_c$  between caustics to grow in time,  $t_c \sim t^{\delta_c}$ , with  $\delta_c = 0.332(3)$ , which is distinctly different from the coarsening of the infrared (IR) length scale of the system, which scales with  $\beta_\Lambda \simeq 1/4$  as a result of the nonlinear interactions, cf. [50]. This leads to the scaling of the correlation length  $\ell_V(t) \sim t^{\beta_V}$  of the effectively random potential  $V(x, t)$  giving rise to the caustics. Analyzing the generation of caustics in a dynamically coarsening random potential, we predict the exponents to be related by  $\delta_c = 4\beta_V/3$ .

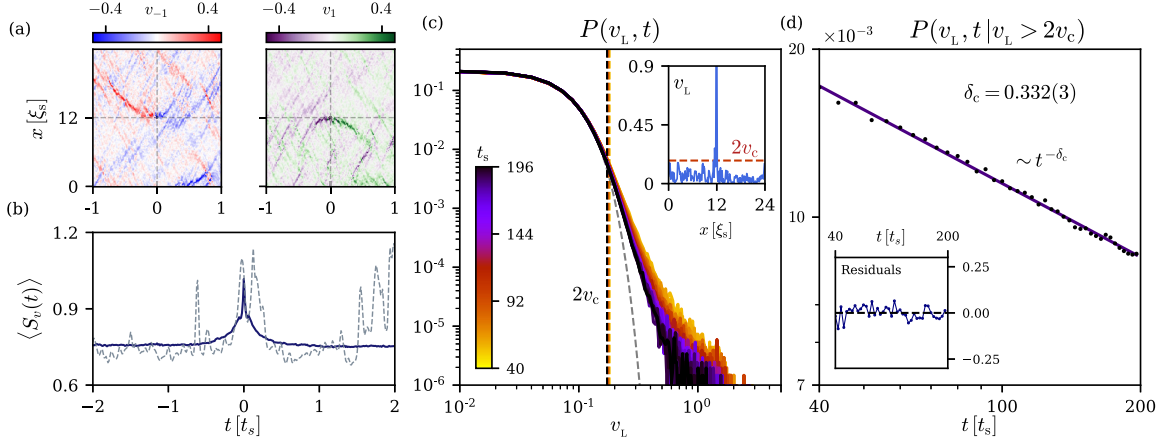


FIG. 1. Characteristics of caustics in the system after a quench. Units are set by the spin healing length  $\xi_s = (2Mn|c_1|)^{-1/2}$  and its corresponding spin-changing collision time  $t_s = 2\pi/(n|c_1|)$ . (a) Excerpt of the space-time evolution of phase defects in the system. The phase gradients  $v_1 = \partial_x \varphi_1$  (purple to green) and  $v_{-1}$  (red to blue) show the formation of rogue-wave-like excitations in the condensate which focus on a singular point marked by the cross. (b) The scintillation index  $S_v(t)$ , Eq. (2), around a rogue wave at  $t = 0$ . The blue solid line shows the scintillation profile averaged over  $\sim 10^3$  (not normalized) rogue waves. The dashed line depicts  $S_v(t)$  for the single truncated Wigner run in (a). (c) PDF of the local Larmor velocity  $v_L = \partial_x \varphi_L = \partial_x(\varphi_1 - \varphi_{-1})$  for different times. The PDF takes the form of a Rayleigh exponential distribution (gray dashed line fit) with a heavy tail. The extreme events are characterized as those with an amplitude larger than  $2v_c$ , where  $v_c$  is the scale velocity, representing the mean of the upper tertile of events. The inset shows that  $v_L > 2v_c$  at the focusing time  $t = 0$ . (d) The probability of finding an extreme event as a function of time. A power law decay  $t^{-\delta_c}$ , with  $\delta_c = 0.332(3)$  is found. The inset shows the deviation of the fit from the data divided by the data point error.

At the focal point of a caustic, a strong phase kink occurs, which can drive the Larmor phase  $\varphi_L = \varphi_1 - \varphi_{-1}$  into the next Riemann sheet, causing a winding-number jump and with this a real-time instanton event. These topological defects are robust, allowing us to differentiate them from the background, making them a reliable probe for the dynamics of the system. We identify these topological defects in the Larmor phase, which take on the form of space-time vortices. The characteristic frequency with which such events occur is found to decay with a power law in time,  $\Gamma \sim t^{-\delta_1}$ , with  $\delta_1 = 0.34(1)$ , corroborating the temporal behavior of caustics. The spatial probability distribution function (PDF) of the corresponding kinks decays exponentially with the distance between them, with the mean distance increasing as  $\langle r \rangle(t) \sim t^{\beta_1}$ , with the exponent  $\beta_1 = 0.26(1)$ , which is consistent with the length-scale coarsening exponent  $\beta_\Lambda$  of the order parameter.

The one-dimensional spin-1 Bose gas is described by the Hamiltonian

$$H = \int dx \left[ \Psi^\dagger \left( -\frac{1}{2M} \frac{\partial^2}{\partial x^2} + qf_z^2 \right) \Psi + \frac{c_0}{2} n^2 + \frac{c_1}{2} |\mathbf{F}|^2 \right], \quad (1)$$

where  $\Psi = (\Psi_1, \Psi_0, \Psi_{-1})^T$  is the three-component bosonic spinor field and  $M$  is the atomic mass. Density-density interactions are described by the term  $c_0 n^2$ , where  $n = \Psi^\dagger \cdot \Psi$  is the total density. Spin changing collisions are contained in the term  $c_1 |\mathbf{F}|^2$ , with  $\mathbf{F} = \Psi^\dagger \mathbf{f} \Psi$  and  $\mathbf{f} = (f_x, f_y, f_z)$  are the generators of the  $\mathfrak{so}(3)$  Lie algebra

in the three-dimensional fundamental representation, cf. Sec. S1C in the Supplemental Material [85], Eq. (S4).  $q$  determines the quadratic Zeeman field strength, which causes an effective shift in the energies of the  $m_F = \pm 1$  components relative to the  $m_F = 0$  component. The linear Zeeman effect is transformed away by considering a rotating frame of reference, i.e., absorbed into the time evolution of the fields.

*Simulations of the dynamics after a quench.*—We consider quenches from the polar ( $c_1 < 0$ ,  $q > 2n|c_1|$ ) to the easy-plane phase ( $c_1 < 0$ ,  $0 < q < 2n|c_1|$ ), where we expect the spin degrees of freedom to be dominantly oriented in the  $F_x$ - $F_y$  plane, see [85], Sec. S1B for details. We prepare the condensate in the mean-field polar phase, which is characterized by a full macroscopic occupation of the  $m_F = 0$  component  $\psi_0(x)/\sqrt{n} = \langle \Psi_0 \rangle / \sqrt{n} = 1$ , while the  $m_F = \pm 1$  magnetic levels are empty. The simulations are performed in an experimentally realistic parameter regime for  $^{87}\text{Rb}$ , i.e.,  $|c_1| \ll c_0$ . We add noise to the Bogoliubov modes of the initial state and quench the quadratic Zeeman shift through the second-order phase transition to a final value of  $q_f = 0.9n|c_1|$ . We propagate this state by means of Truncated-Wigner simulations with periodic boundary conditions, see [85], Sec. S1C for more details. Following the quench, instabilities lead to a fast buildup of strong excitations in the relative phases between the different magnetic components, which reflect spatial redistributions of bosons under the interaction-induced constraint of a nearly constant total density  $n$ , i.e., due to  $|c_1| \ll c_0$  [50].

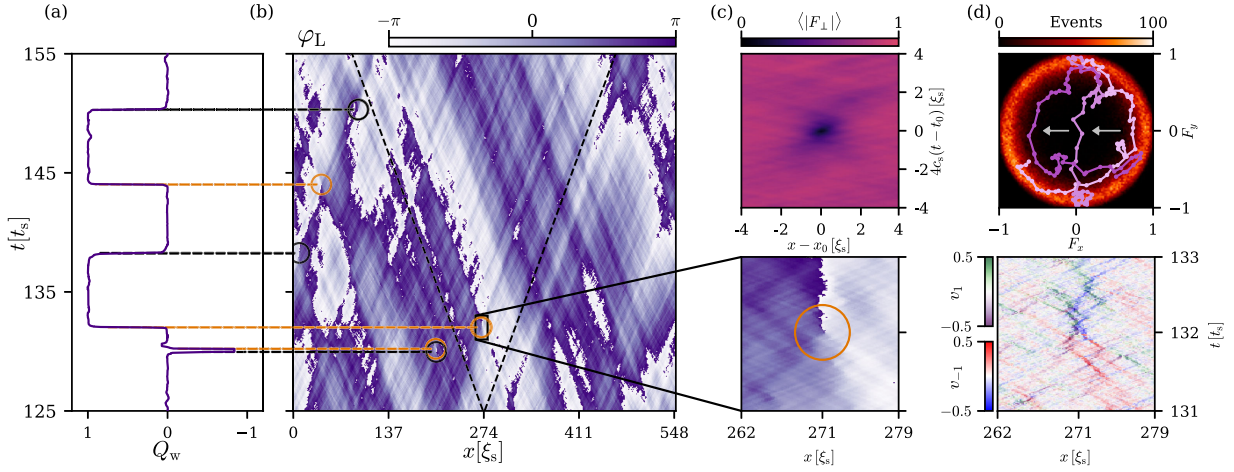


FIG. 2. Structures and defects in the time evolution of the Larmor phase after a quench (units chosen as in Fig. 1). (a) Time evolution of the winding number  $Q_w$  for the run shown in panel (b). (b) Space-time evolution of the Larmor phase of the transversal spin  $F_\perp = |F_\perp| \exp[i\varphi_L]$  across the entire system in a single truncated-Wigner (TW) run, with the spin speed of sound  $c_s = \sqrt{n|c_1|}/2M$  (dashed line). In the strongly fluctuating system, vortex structures in space and time are observed, as the phase wraps around one point [cf. zoom in panel (c)]. Instantons (orange) and anti-instantons (black), each cause an integer jump in the winding number  $Q_w(t)$ . (c) Structure of the real-time instanton. In the upper panel, the averaged  $|F_\perp|$  profile of a defect located at  $x_0$  at time  $t_0$  is depicted. The lower panel shows the vortexlike nature of the defect in more detail, around which the Larmor phase winds by  $2\pi$ . (d) The lower panel shows the corresponding intersection of two rogue waves in  $v_{\pm 1}$  at the position of the instanton, recall Fig. 1(a). The upper panel exhibits the temporal evolution (bright to dark pink) of the  $F_\perp$  field configuration in spin space, within the window shown in the lower panels. The outer circle represents a histogram (black to bright red color code) of spin orientations in the  $F_x$ - $F_y$  plane averaged over 100 TW runs.

*Caustics.*—The highly excited system in its postquench time evolution is observed to generate focusing of the magnetic excitations into momentaneous rogue waves in the  $m_F = 0$  density, giving rise to density dips in the  $m_F = \pm 1$  modes, and thus to rogue-wave-like peaks in the velocity fields  $v_{m_F} \sim \partial_x \varphi_{m_F}$  in Fig. 1(a) (cf. Fig. S2 in [85]). These rogue waves can be characterized as caustics [73–77], which are signaled by the scintillation index

$$S_v(t) = \frac{\langle |v_L|^2 \rangle_x}{\langle |v_L| \rangle_x^2} - 1 \quad (2)$$

as rare extreme events in the velocity fields, where  $\langle \dots \rangle_x$  denotes the spatial average and  $v_L = \partial_x \varphi_L = v_1 - v_{-1}$ . At times where the system shows strong phase kinks, we expect a strong sudden rise in the scintillation index [see Fig. 1(b)].

To study the coarsening dynamics of caustics, we investigate the probability distribution function (PDF) of velocities associated with caustics, which is known to be long tailed [90–93], as is confirmed by our simulations, see Fig. 1(c). The PDF of velocities follows a heavy-tailed Rayleigh exponential form (cf. Fig. S3 in [85]), implying that the dynamics are driven by coherent wave packets [76]. One obtains a scale *velocity of significant waves*,  $v_c$ , as the mean of the upper tertile of the PDF. The criterion for rogue waves is then chosen to include those with an amplitude  $v_L > 2v_c$  [92]. Figure 1(d) shows that the probability of

such rare events to occur decays with a power law,  $P(v_L, t | v_L > 2v_c) \sim t^{-\delta_c}$ , with  $\delta_c = 0.332(3)$ .

The underlying timescale of caustic focusing and appearance of rogue or freak wave excitations can be described in the framework of a stochastic nonlinear Schrödinger equation (NLSE) [79–81]. To investigate the temporal behavior of extreme events in our system, we consider the equations of motion for  $\Psi$ ,

$$i\partial_t \Psi = \left[ -\frac{\partial_x^2}{2M} + qf_z^2 + c_0 n + c_1 \mathbf{F} \cdot \mathbf{f} \right] \Psi. \quad (3)$$

Because of the strong density-density interactions and the disordered behavior of the spin-changing term, the last term of Eq. (3) can be considered as a fluctuating weak random potential  $V(x, t) \equiv c_1 \mathbf{F}(x, t) \cdot \mathbf{f}$  added to a NLSE. Our numerical simulations show that  $\langle V \rangle = 0$ , since, in the mean over many realizations, the SO(2) symmetry is restored in the easy plane, and  $\langle F_z \rangle = 0$ . Yet, we obtain exponential correlations in the diagonal elements  $\langle \text{Tr}[V(x, t)V(0, 0)] \rangle = V_0^2 \exp[-x/\ell_V(t)]$ , with strength  $V_0$  and a correlation length scale  $\ell_V$ , whereas the off-diagonal elements of the correlation vanish, see [85], Sec. S2B for details.

For a propagation in random media, the time needed for the waves to focus, i.e., the *mean time to caustics*  $t_c$ , depends only on the correlation length  $\ell_V$  of the random medium and on the strength  $V_0$  of the fluctuations [73–77]. In contrast to the standard case studied in the context of

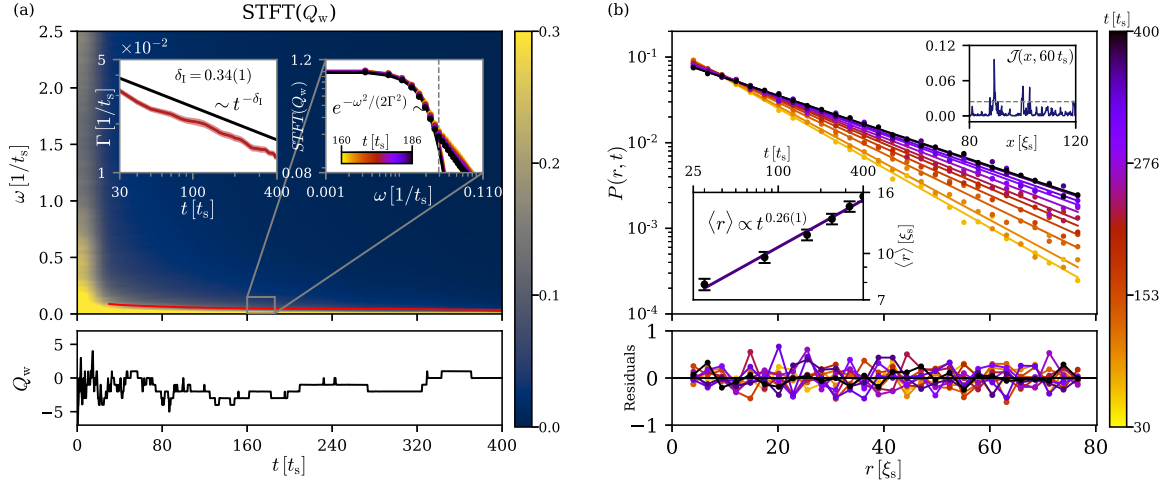


FIG. 3. Statistics of the instantons after a quench. (a) Short-time Fourier transform (STFT) of the winding number  $Q_w(t)$  (main panel, color scale), exhibiting a Gaussian fall-off for small frequencies (up to the gray dashed line in the right inset)  $\text{STFT}[Q_w](t) \sim \exp\{-\omega^2/[2\Gamma^2(t)]\}$  (right inset), with width decreasing as  $\Gamma(t) \sim t^{-\delta_1}$ ,  $\delta_1 = 0.34(1)$  (left inset and red line in main panel), confirming power-law coarsening dynamics of the governing timescale of  $Q_w$ . The lower panel shows the time evolution of the winding number  $Q_w$  for a single realization. (b) The PDF of spatial defect separation is found to fall off exponentially,  $P(r, t) \sim A(t) \exp[-r/\zeta(t)]$ , with mean distance  $\langle r \rangle(t) \sim t^{\beta_1}$ , increasing from early times (yellow) to later times (black), exhibiting power-law coarsening with exponent  $\beta_1 = 0.26(1)$  (lower inset). The upper inset shows the chosen threshold of the current  $\mathcal{J}(x, t) = |\partial_x \varphi_L| \cdot (\langle |F_\perp| \rangle_x - |F_\perp|)$  for defect detection which corresponds to the top decile of amplitude. The lower panel shows the difference of the data to the fit function divided by the standard deviation of each data point.

caustics, the intricate nonlinear interactions between the components of the condensate cause the correlation length to dynamically scale in time. Our numerical simulations confirm the scaling of the correlation length of the noise term in Eq. (3) as  $\ell_V(t) \sim t^{\beta_V}$ , with  $\beta_V = 0.252(3)$ , cf. [85], S2A and S2B. Generalizing the arguments used in [74] to Bogoliubov modes, one finds the mean time to caustics to scale as  $t_c \sim \ell_V^{A/3}$ , for details see [85], S2B. Thus, a temporally growing correlation length  $\ell_V(t) \sim t^{\beta_V}$ , with  $\beta_V \simeq 1/4$ , implies that the mean time to caustics scales in time as  $t_c \sim t^{\delta_c}$ , with  $\delta_c = 4\beta_V/3 \simeq 1/3$ .

The observed power-law coarsening indicates a close connection with the spatiotemporal scaling of the structure factor  $S_{F_\perp}(t, p) = \langle F_\perp(t, p)^\dagger F_\perp(t, p) \rangle$  of the transverse spin  $F_\perp \equiv F_x + iF_y = |F_\perp| \exp[i\varphi_L]$  as found in [50] (cf. [85], Sec. S2A),

$$S_{F_\perp}(t, p) = (t/t_{\text{ref}})^\alpha f_s([t/t_{\text{ref}}]^\beta p). \quad (4)$$

Here  $f_s$  is a universal scaling function, which depends only on the momentum  $p$ ,  $t_{\text{ref}}$  is a reference time within the scaling interval, and the scaling exponents  $\alpha = 0.27(6)$  and  $\beta = 0.25(4)$  are, within errors, related by  $\alpha = d\beta$ ,  $d = 1$ , ensuring the momentum integral over  $S_{F_\perp}(t, p)$  to be conserved. The scaling is a manifestation of the coarsening of an infrared correlation scale, growing as  $\ell_\Lambda \sim t^{\beta_\Lambda}$ , which in turn gives rise to the algebraic increase of the noise correlation length scale  $\ell_V$  with the same exponent,  $\beta_V \simeq \beta_\Lambda$ , as is confirmed within errors by our simulations.

*Real-time instantons in the Larmor phase.*—In the emerging postquench dynamics, the confluence of rogue-wave excitations in the velocity fields  $v_{\pm 1}$  manifests itself as an interplay of strong phase kinks in  $\Psi_{\pm 1}$ . Analyzing the propagation of the velocity fields over many realizations reveals that the encounter of two focused waves with opposite signs, each in a different component [Fig. 1(a)], results in an overall phase jump in the Larmor phase, forcing  $\varphi_L$  into the next Riemann sheet. As a result, the Larmor phase changes its overall winding number across the system [Figs. 2(a) and 2(b)], an event which we refer to as a *real-time instanton*. Instantons are of strong relevance in fundamental studies of quantum field theory and matter [94,95], as well as various applications, including false vacuum decay [96–98]. Phenomena closely related to the real-time instantons we study here include coherence vortices [99] and phase slips [100–104].

As can be seen in the lower panel of Fig. 2(c), a vortex-type defect occurs in the Larmor phase, at a time  $t \simeq 132t_s$  and position  $x \simeq 271\xi_s$ , at the intersection of phase kinks, where a strong rogue-wave excitation occurs. In Fig. 2(d) (upper), the instanton defect is seen to result from the field configuration crossing in time the center of the transversal spin plane, causing a local spin length reduction. As a result, the phase wraps into the next Riemann sheet, giving rise to a change of the overall winding number of the Larmor phase,

$$Q_w = \frac{1}{2\pi} \int_0^{\mathcal{L}} dx \partial_x \varphi_L \in \mathbb{Z}, \quad (5)$$

where  $\mathcal{L}$  is the system's length. With the help of a plaquette algorithm correlating jumps in the Larmor phase and dips in the spin length, we localize the instantons in space and time.

During the evolution of the system following the quench, the density of (anti-)instantons decreases, and the probability of the system producing a topological defect reduces as it attempts to settle to a state with constant winding number, see the lower panel of Fig. 3(a). The robustness of these topological defects enables us to distinguish them from the background. To extract the instanton probability decay, we perform a short-time Fourier transform (STFT) of  $Q_w(t)$  over time windows of width  $\Delta t_{\text{STFT}} = 70t_s$ . The resulting STFT[ $Q_w$ ]( $t, \omega$ ) is shown in Fig. 3(a). At each time, the winding number jump frequencies display an approximate Gaussian fall-off  $\exp\{-\omega^2/[2\Gamma^2(t)]\}$ , with scale  $\Gamma$  which is extracted via a least-squares fit and found to decrease in time as  $\Gamma(t) \sim t^{-\delta_I}$ , with  $\delta_I = 0.34(1)$  [insets of Fig. 3(a)]. This confirms the scaling of the mean time to caustics within the error bounds.

To investigate the underlying spatial coarsening of the system, we recall the vortex structures shown in Fig. 2 giving rise to a length scale in  $\varphi_L$ . In Fig. 3(b), we depict the distribution spatial instanton separation in the system. The resulting PDF exhibits an exponential fall-off  $P(r, t) \sim A(t) \exp[-r/\zeta(t)]$  with the mean separation increasing as  $\langle r \rangle(t) = \int dr r P(r, t) \sim t^{\beta_I}$  with exponent  $\beta_I = 0.26(1)$ , cf. the lower inset of Fig. 3(b), corroborating the results obtained in [50]. Hence, within the error bounds, the relation  $\delta_c = 4\beta_V/3$  holds in the spatiotemporal scaling of the real-time instantons, which introduce a scale into the order parameter  $F_\perp$ .

**Conclusions.**—Quenching a one-dimensional spin-1 Bose gas into the easy-plane phase leads to rich dynamics in the  $F_x$ - $F_y$  plane reflected in the fluctuations of the Larmor phase  $\varphi_L$ . Rare extreme rogue waves emerge from the disordered dynamics, which act as an effective random potential with a time varying correlation length  $\ell_V(t)$  on the different components of the spinor gas. The timescale set by these events is found to scale as  $t_c \sim t^{4\beta_V/3} \sim t^{1/3}$ , which corroborates the coarsening dynamics of the spin correlations. The focusing events give rise to real-time instantons, i.e., vortex structures in space and time in the Larmor phase, which in turn introduce the coarsening length scale found in the power spectrum of  $F_\perp$ . These defects occur with algebraically decaying probability in time, reflecting, once more, a temporally coarsening timescale  $\Gamma \sim t_c^{-1} \sim t^{-1/3}$ . Our results open a perspective on studying caustics [68–72] leading to rogue waves [73–77] in multicomponent Bose condensates. Two exponents  $\beta \equiv \beta_V \simeq \beta_\Lambda \simeq \beta_I$  and  $\delta \equiv \delta_c \simeq \delta_I$  emerge, reflecting a different algebraic growth in time, of the length scale and timescale, respectively, which are connected by  $\delta = 4\beta/3$ . The type of nonthermal fixed point observed

in the multicomponent field model could bear interesting consequences for universal dynamics in the context of other systems, ranging from structure formation in the Universe to nonlinear hydrodynamics and microscopic physics.

The authors thank V. Bagnato, J. Berges, J. Bloch, A. Bulgac, K. Geier, P. Große-Bley, P. Heinen, M. Karl, W. Kirkby, A. N. Mikheev, R. Miyar, J. M. Pawłowski, A. Piñeiro Orioli, M. Prüfer, N. Rasch, C. M. Schmied, T. Simula, and S. K. Turitsyn for discussions and collaboration on related topics. They acknowledge support by the ERC Advanced Grant EntangleGen (Project-ID 694561), by the German Research Foundation (Deutsche Forschungsgemeinschaft, DFG), through SFB 1225 ISOQUANT (Project-ID 273811115), Grant No. GA677/10-1, and under Germany's Excellence Strategy—EXC 2181/1–390900948 (the Heidelberg STRUCTURES Excellence Cluster), and by the state of Baden-Württemberg through bwHPC and DFG through Grants No. INST 35/1134-1 FUGG, No. INST 35/1503-1 FUGG, No. INST 35/1597-1 FUGG, and No. 40/575-1 FUGG.

\*t.gasenzner@uni-heidelberg.de

- [1] J. Berges, S. Borsanyi, and C. Wetterich, *Phys. Rev. Lett.* **93**, 142002 (2004).
- [2] T. Langen, T. Gasenzner, and J. Schmiedmayer, *J. Stat. Mech.* (2016) 064009.
- [3] V. E. Zakharov, V. S. L'vov, and G. Falkovich, *Kolmogorov Spectra of Turbulence I: Wave Turbulence* (Springer, Berlin, 1992).
- [4] S. Nazarenko, *Wave turbulence*, Lecture Notes in Physics Vol. 825 (Springer, Heidelberg, 2011), pp. XVI, 279 S.
- [5] W. Vinen, *J. Low Temp. Phys.* **145**, 7 (2006).
- [6] M. Tsubota, *J. Phys. Soc. Jpn.* **77**, 111006 (2008).
- [7] J. Berges, A. Rothkopf, and J. Schmidt, *Phys. Rev. Lett.* **101**, 041603 (2008).
- [8] J. Schole, B. Nowak, and T. Gasenzner, *Phys. Rev. A* **86**, 013624 (2012).
- [9] A. Piñeiro Orioli, K. Boguslavski, and J. Berges, *Phys. Rev. D* **92**, 025041 (2015).
- [10] I. Chantesana, A. P. Orioli, and T. Gasenzner, *Phys. Rev. A* **99**, 043620 (2019).
- [11] A. N. Mikheev, C.-M. Schmied, and T. Gasenzner, *Phys. Rev. A* **99**, 063622 (2019).
- [12] E. A. L. Henn, J. A. Seman, G. Roati, K. M. F. Magalhães, and V. S. Bagnato, *Phys. Rev. Lett.* **103**, 045301 (2009).
- [13] M. Gring, M. Kuhnert, T. Langen, T. Kitagawa, B. Rauer, M. Schreitl, I. Mazets, D. A. Smith, E. Demler, and J. Schmiedmayer, *Science* **337**, 1318 (2012).
- [14] D. A. Smith, M. Gring, T. Langen, M. Kuhnert, B. Rauer, R. Geiger, T. Kitagawa, I. Mazets, E. Demler, and J. Schmiedmayer, *New J. Phys.* **15**, 075011 (2013).
- [15] T. Langen, S. Erne, R. Geiger, B. Rauer, T. Schweigler, M. Kuhnert, W. Rohringer, I. E. Mazets, T. Gasenzner, and J. Schmiedmayer, *Science* **348**, 207 (2015).

- [16] N. Navon, A. L. Gaunt, R. P. Smith, and Z. Hadzibabic, *Science* **347**, 167 (2015).
- [17] N. Navon, A. L. Gaunt, R. P. Smith, and Z. Hadzibabic, *Nature (London)* **539**, 72 (2016).
- [18] B. Rauer, S. Erne, T. Schweigler, F. Cataldini, M. Tajik, and J. Schmiedmayer, *Science* **360**, 307 (2018).
- [19] G. Gauthier, M. T. Reeves, X. Yu, A. S. Bradley, M. A. Baker, T. A. Bell, H. Rubinsztein-Dunlop, M. J. Davis, and T. W. Neely, *Science* **364**, 1264 (2019).
- [20] S. P. Johnstone, A. J. Groszek, P. T. Starkey, C. J. Billington, T. P. Simula, and K. Helmerson, *Science* **364**, 1267 (2019).
- [21] C. Eigen, J. A. P. Glidden, R. Lopes, E. A. Cornell, R. P. Smith, and Z. Hadzibabic, *Nature (London)* **563**, 221 (2018).
- [22] M. Prüfer, P. Kunkel, H. Strobel, S. Lannig, D. Linnemann, C.-M. Schmied, J. Berges, T. Gasenzer, and M. K. Oberthaler, *Nature (London)* **563**, 217 (2018).
- [23] S. Erne, R. Bücker, T. Gasenzer, J. Berges, and J. Schmiedmayer, *Nature (London)* **563**, 225 (2018).
- [24] N. Navon, C. Eigen, J. Zhang, R. Lopes, A. L. Gaunt, K. Fujimoto, M. Tsubota, R. P. Smith, and Z. Hadzibabic, *Science* **366**, 382 (2019).
- [25] J. A. P. Glidden, C. Eigen, L. H. Dogra, T. A. Hilker, R. P. Smith, and Z. Hadzibabic, *Nat. Phys.* **17**, 457 (2021).
- [26] A. D. García-Orozco, L. Madeira, M. A. Moreno-Armijos, A. R. Fritsch, P. E. S. Tavares, P. C. M. Castilho, A. Cidrim, G. Roati, and V. S. Bagnato, *Phys. Rev. A* **106**, 023314 (2022).
- [27] T. Kodama, H. T. Elze, C. E. Aguiar, and T. Koide, *Europhys. Lett.* **70**, 439 (2005).
- [28] R. Barnett, A. Polkovnikov, and M. Vengalattore, *Phys. Rev. A* **84**, 023606 (2011).
- [29] M. Marcuzzi, J. Marino, A. Gambassi, and A. Silva, *Phys. Rev. Lett.* **111**, 197203 (2013).
- [30] T. Langen, M. Gring, M. Kuhnert, B. Rauer, R. Geiger, D. A. Smith, I. E. Mazets, and J. Schmiedmayer, *Eur. Phys. J. Special Topics* **217**, 43 (2013).
- [31] N. Nesi, A. Iucci, and M. A. Cazalilla, *Phys. Rev. Lett.* **113**, 210402 (2014).
- [32] P. Gagel, P. P. Orth, and J. Schmalian, *Phys. Rev. Lett.* **113**, 220401 (2014).
- [33] B. Bertini, F. H. L. Essler, S. Groha, and N. J. Robinson, *Phys. Rev. Lett.* **115**, 180601 (2015).
- [34] M. Babadi, E. Demler, and M. Knap, *Phys. Rev. X* **5**, 041005 (2015).
- [35] M. Buchhold, M. Heyl, and S. Diehl, *Phys. Rev. A* **94**, 013601 (2016).
- [36] J. Berges and G. Hoffmeister, *Nucl. Phys.* **B813**, 383 (2009).
- [37] B. Nowak, J. Schole, and T. Gasenzer, *New J. Phys.* **16**, 093052 (2014).
- [38] J. Hofmann, S. S. Natu, and S. Das Sarma, *Phys. Rev. Lett.* **113**, 095702 (2014).
- [39] A. Maraga, A. Chiocchetta, A. Mitra, and A. Gambassi, *Phys. Rev. E* **92**, 042151 (2015).
- [40] L. A. Williamson and P. B. Blakie, *Phys. Rev. Lett.* **116**, 025301 (2016).
- [41] L. A. Williamson and P. B. Blakie, *Phys. Rev. A* **94**, 023608 (2016).
- [42] A. Bourges and P. B. Blakie, *Phys. Rev. A* **95**, 023616 (2017).
- [43] A. Chiocchetta, A. Gambassi, S. Diehl, and J. Marino, *Phys. Rev. B* **94**, 174301 (2016).
- [44] M. Karl and T. Gasenzer, *New J. Phys.* **19**, 093014 (2017).
- [45] A. Schachner, A. Piñeiro Orioli, and J. Berges, *Phys. Rev. A* **95**, 053605 (2017).
- [46] R. Walz, K. Boguslavski, and J. Berges, *Phys. Rev. D* **97**, 116011 (2018).
- [47] C.-M. Schmied, A. N. Mikheev, and T. Gasenzer, *Phys. Rev. Lett.* **122**, 170404 (2019).
- [48] C.-M. Schmied, A. N. Mikheev, and T. Gasenzer, *Int. J. Mod. Phys. A* **34**, 1941006 (2019).
- [49] A. Mazeliauskas and J. Berges, *Phys. Rev. Lett.* **122**, 122301 (2019).
- [50] C.-M. Schmied, M. Prüfer, M. K. Oberthaler, and T. Gasenzer, *Phys. Rev. A* **99**, 033611 (2019).
- [51] L. A. Williamson and P. B. Blakie, *SciPost Phys.* **7**, 029 (2019).
- [52] C. M. Schmied, T. Gasenzer, and P. B. Blakie, *Phys. Rev. A* **100**, 033603 (2019).
- [53] C. Gao, M. Sun, P. Zhang, and H. Zhai, *Phys. Rev. Lett.* **124**, 040403 (2020).
- [54] M. T. Wheeler, H. Salman, and M. O. Borgh, *Europhys. Lett.* **135**, 30004 (2021).
- [55] L. Gresista, T. V. Zache, and J. Berges, *Phys. Rev. A* **105**, 013320 (2022).
- [56] J. F. Rodríguez-Nieva, A. Piñeiro Orioli, and J. Marino, *Proc. Natl. Acad. Sci. U.S.A.* **119**, e2122599119 (2021).
- [57] T. Preis, M. P. Heller, and J. Berges, *Phys. Rev. Lett.* **130**, 031602 (2023).
- [58] I.-K. Liu, N. P. Proukakis, and G. Rigopoulos, *Mon. Not. R. Astron. Soc.* **521**, 3625 (2023).
- [59] P. Heinen, A. N. Mikheev, C.-M. Schmied, and T. Gasenzer, *arXiv:2212.01162*.
- [60] P. Heinen, A. N. Mikheev, and T. Gasenzer, *Phys. Rev. A* **107**, 043303 (2023).
- [61] P. C. Hohenberg and B. I. Halperin, *Rev. Mod. Phys.* **49**, 435 (1977).
- [62] H. Janssen, in *Dynamical Critical Phenomena and Related Topics*, Lecture Notes in Physics Vol. 104 (Springer, Heidelberg, 1979), p. 26.
- [63] H. W. Diehl, in *Phase Transitions and Critical Phenomena* (Academic Press, London, 1986).
- [64] H. Janssen, in *From Phase Transitions to Chaos* (World Scientific, Singapore, 1992), p. 68.
- [65] A. J. Bray, *Adv. Phys.* **43**, 357 (1994).
- [66] *Kinetics of Phase Transitions*, edited by S. Puri and V. Wadhawan (Taylor & Francis Group, Boca Raton, 2009).
- [67] L. F. Cugliandolo, *C.R. Phys.* **16**, 257 (2015).
- [68] M. V. Berry, *J. Phys. A* **10**, 2061 (1977).
- [69] M. V. Berry, *J. Phys. A* **10**, 2083 (1977).
- [70] J. Mumford, W. Kirkby, and D. H. J. O'Dell, *J. Phys. B* **50**, 044005 (2017).
- [71] W. Kirkby, J. Mumford, and D. H. J. O'Dell, *Phys. Rev. Res.* **1**, 033135 (2019).
- [72] W. Kirkby, Y. Yee, K. Shi, and D. H. J. O'Dell, *Phys. Rev. Res.* **4**, 013105 (2022).

- [73] J. J. Metzger, R. Fleischmann, and T. Geisel, *Phys. Rev. Lett.* **112**, 203903 (2014).
- [74] L. Kaplan, *Phys. Rev. Lett.* **89**, 184103 (2002).
- [75] J. J. Metzger, R. Fleischmann, and T. Geisel, *Phys. Rev. Lett.* **105**, 020601 (2010).
- [76] J. J. Metzger, R. Fleischmann, and T. Geisel, *Phys. Rev. Lett.* **111**, 013901 (2013).
- [77] H. Degueldre, J. J. Metzger, T. Geisel, and R. Fleischmann, *Nat. Phys.* **12**, 259 (2016).
- [78] F. T. Arecchi, U. Bortolozzo, A. Montina, and S. Residori, *Phys. Rev. Lett.* **106**, 153901 (2011).
- [79] L. H. Ying and L. Kaplan, *J. Geophys. Res. Oceans* **117**, C08016 (2012).
- [80] M. Onorato, S. Residori, U. Bortolozzo, A. Montina, and F. Arecchi, *Phys. Rep.* **528**, 47 (2013).
- [81] G. Green and R. Fleischmann, *New J. Phys.* **21**, 083020 (2019).
- [82] N. Akhmediev and E. Pelinovsky, *Eur. Phys. J. Special Topics* **185**, 1 (2010).
- [83] Y. V. Bludov, V. V. Konotop, and N. Akhmediev, *Phys. Rev. A* **80**, 033610 (2009).
- [84] Y. Kawaguchi and M. Ueda, *Phys. Rep.* **520**, 253 (2012).
- [85] See Supplemental Material at <http://link.aps.org/supplemental/10.1103/PhysRevLett.131.183402> for further details on numerical simulations and analytical methods, which includes Refs. [86–89].
- [86] P. B. Blakie, A. S. Bradley, M. J. Davis, R. J. Ballagh, and C. W. Gardiner, *Adv. Phys.* **57**, 363 (2008).
- [87] A. Polkovnikov, *Ann. Phys. (Amsterdam)* **325**, 1790 (2010).
- [88] S. Lannig, M. Prüfer, Y. Deller, I. Siovitz, J. Dreher, T. Gasenzer, H. Strobel, and M. K. Oberthaler, [arXiv:2306.16497](https://arxiv.org/abs/2306.16497).
- [89] Here we introduce a notation which distinguishes the exponent  $\beta_1$  characterizing the length scale associated with instantons as compared to the general  $\beta$  characterizing the coarsening (4) of the structure factor, in order to not mangle our results upfront. As it turns out,  $\beta_1$  and  $\beta$  cannot be distinguished within our numerical accuracy and are expected to be equivalent to each other.
- [90] A. Safari, R. Fickler, M. J. Padgett, and R. W. Boyd, *Phys. Rev. Lett.* **119**, 203901 (2017).
- [91] A. Mathis, L. Froehly, S. Toenger, F. Dias, G. Genty, and J. M. Dudley, *Sci. Rep.* **5**, 12822 (2015).
- [92] J. M. Dudley, F. Dias, M. Erkintalo, and G. Genty, *Nat. Photonics* **8**, 755 (2014).
- [93] D. R. Solli, C. Ropers, P. Koonath, and B. Jalali, *Nature (London)* **450**, 1054 (2007).
- [94] N. Seiberg and E. Witten, *Nucl. Phys.* **B426**, 19 (1994); **B430**, 485(E) (1994).
- [95] N. Seiberg and E. Witten, *Nucl. Phys.* **B431**, 484 (1994).
- [96] S. W. Hawking, I. G. Moss, and J. M. Stewart, *Phys. Rev. D* **26**, 2681 (1982).
- [97] J. Braden, J. R. Bond, and L. Mersini-Houghton, *J. Cosmol. Astropart. Phys.* **03** (2015) 007.
- [98] J. R. Bond, J. Braden, and L. Mersini-Houghton, *J. Cosmol. Astropart. Phys.* **09** (2015) 004.
- [99] T. P. Simula and D. M. Paganin, *Phys. Rev. A* **84**, 052104 (2011).
- [100] H. P. Büchler, V. B. Geshkenbein, and G. Blatter, [arXiv: cond-mat/9911301](https://arxiv.org/abs/cond-mat/9911301).
- [101] I. Danshita and A. Polkovnikov, *Phys. Rev. A* **85**, 023638 (2012).
- [102] I. Danshita, *Phys. Rev. Lett.* **111**, 025303 (2013).
- [103] C. D’Errico, S. S. Abbate, and G. Modugno, *Phil. Trans. Act. R. Soc. A* **375**, 20160425 (2017).
- [104] J. Polo, R. Dubessy, P. Pedri, H. Perrin, and A. Minguzzi, *Phys. Rev. Lett.* **123**, 195301 (2019).